IOPscience iopscience.iop.org

Home Search Collections Journals About Contact us My IOPscience

Normal-state conductance used to probe superconducting tunnel junctions for quantum computing

This article has been downloaded from IOPscience. Please scroll down to see the full text article.

2010 Supercond. Sci. Technol. 23 045002

(http://iopscience.iop.org/0953-2048/23/4/045002)

The Table of Contents and more related content is available

Download details:
IP Address: 132.163.130.151
The article was downloaded on 24/03/2010 at 20:44

Please note that terms and conditions apply.

Supercond. Sci. Technol. **23** (2010) 045002 (7pp) doi:10.1088/0953-2048/23/4/045002

Normal-state conductance used to probe superconducting tunnel junctions for quantum computing

Carlos Chaparro[1], Richard Bavier[1], Yong-Seung Kim[1], Eunyoung Kim[1], Jeffrey S Kline[2], David P Pappas[2] and Seongshik Oh[1]

[1] Department of Physics and Astronomy, Rutgers, The State University of New Jersey, Piscataway, NJ 08854, USA
[2] National Institute of Standards and Technology, Boulder, CO 80305, USA

E-mail: carlosch@physics.rutgers.edu and ohsean@physics.rutgers.edu

Received 4 November 2009, in final form 15 December 2009
Published 3 March 2010
Online at stacks.iop.org/SUST/23/045002

Abstract
Here we report normal-state conductance measurements of three different types of superconducting tunnel junctions that are being used or proposed for quantum computing applications: p-Al/a-AlO/p-Al, e-Re/e-AlO/p-Al, and e-V/e-MgO/p-V, where p stands for polycrystalline, e for epitaxial, and a for amorphous. All three junctions exhibited significant deviations from the parabolic behavior predicted by the WKB approximation models. In the p-Al/a-AlO/p-Al junction, we observed enhancement of tunneling conductances at voltages matching harmonics of Al–O stretching modes. On the other hand, such Al–O vibration modes were missing in the epitaxial e-Re/e-AlO/p-Al junction. This suggests that absence or existence of the Al–O stretching mode might be related to the crystallinity of the AlO tunnel barrier and the interface between the electrode and the barrier. In the e-V/e-MgO/p-V junction, which is one of the candidate systems for future superconducting qubits, we observed suppression of the density of states at zero bias. This implies that the interface is electronically disordered, presumably due to oxidation of the vanadium surface underneath the MgO barrier, even if the interface was structurally well ordered, suggesting that the e-V/e-MgO/p-V junction will not be suitable for qubit applications in its present form. This also demonstrates that the normal-state conductance measurement can be effectively used to screen out low quality samples in the search for better superconducting tunnel junctions.

(Some figures in this article are in colour only in the electronic version)

1. Introduction

Metal–insulator–metal (MIM) tunneling junctions have been the subject of intense investigation from the 1960s [1] to the present search for optimal materials for superconducting qubits [2–4] in quantum computing or for magnetoresistive random-access-memory devices [5, 6].

The trapezoidal barrier model combined with Wentzel–Kramers–Brillouin (WKB)-based approximations, like the Simmons equation [7–9] or the Brinkman–Dynes–Rowell (BDR) [10] approximation, have been a standard model for the description of the tunneling phenomena in MIM junctions. These models predict a parabolic behavior for the differential conductance of MIM junctions near zero bias, by assuming perfectly sharp boundaries, rectangular or trapezoidal barriers, and absolute-zero temperature for calculational simplicity. They have been used extensively to obtain tunnel barrier parameters such as effective thickness or potential barrier height for tunnel junctions. However, parameters obtained by these models sometimes can be physically unreasonable, which can be attributed to the oversimplifications of the barrier. In real junctions, factors such as interfacial roughness, thermal smearing, existence of pinholes, and the crystalline structure of the materials, result in deviations from the ideal model [11, 12].

 © 2010 IOP Publishing Ltd Printed in the UK & the USA

One of the well-known examples that demonstrate the breakdown of WKB models is the zero bias anomaly (ZBA): a narrow peak or dip that appears in the characteristic tunneling conductance behavior as a function of voltage around zero bias [13, 14]. This anomaly near zero bias has been known for a long time [15–19]; it starts to develop at temperatures significantly below room temperature and tends to get more pronounced as absolute zero is approached. Such ZBAs can result from electron–electron interactions [13, 20, 21] or from suppression of the tunneling density of states [20, 22] in the presence of disorder at the interface. None of these are taken into account in the WKB-based models.

In this work we studied the normal-state properties of superconducting tunnel junctions with magnesium and aluminum oxide tunnel barriers: the two most important tunnel barriers for the present and near-future superconducting qubit circuits [23]. Epitaxial MgO and AlO tunnel barriers are expected to overcome the limitations of amorphous AlO tunnel barriers [2, 3, 24] in quantum computation applications. Although the most popular system for superconducting qubits is still p-Al/a-AlO/p-Al tunnel junctions, they suffer from a strong decoherence mechanism, two-level fluctuators [4], originating from the amorphous tunnel barrier and its interface with the electrodes. This observation previously led to the development of a new tunnel junction system, e-Re/e-AlO/p-Al, which demonstrated significant improvement in qubit performance compared to the conventional p-Al/a-AlO/p-Al qubit [2, 3, 24]. Even after this proof-of-concept demonstration, however, the search for new and better superconducting tunnel junctions has been almost dormant, partly due to the big gap between the qubit and the materials research communities. Among other things, while testing qubits requires sophisticated protocols at dilution refrigerator temperatures, most materials research groups do not have easy access to such capabilities. In this work, we show that simple normal-state conductance measurement above liquid helium temperatures can still provide important information for superconducting tunnel junctions. Utilizing such a simple characterizing scheme for pre-screening purposes will also help reduce the turnaround time in the materials search for new superconducting qubits.

In order to see if we can correlate the normal-state properties of superconducting tunnel junctions with their qubit and superconducting properties, we examined three different types of tunnel junctions: p-Al/a-AlO/p-Al, e-Re/e-AlO/p-Al, and e-V/e-MgO/p-V. Each of these three systems holds a unique standing in recent qubit investigations. The first one is, as we discussed above, still the most popular system in the present qubit community, and the second is so far the only system that showed enhanced coherence properties compared to the first [2, 23]. Accordingly, comparing the normal-state properties of these two types will provide a good starting place for future studies of new materials. Although the e-Re/e-AlO/p-Al system demonstrated enhanced coherence properties by significantly reducing the number of two-level fluctuators in the tunnel barrier, it still has a number of other issues that need to be improved. First of all, as reported previously [3, 23], it suffers from significant non-uniformity of junction resistance values, which makes it difficult to adapt to a multi-qubit environment that requires uniform junction resistance for many junctions. Second, the top layer is still non-epitaxial, and we believe that the interface between the top layer and the tunnel barrier probably is responsible for the residual two-level fluctuators [3]. Any attempt to replace the top layer by Re, whether epitaxial or not, resulted in a high subgap leakage current. This observation motivated us to investigate a new type of tunnel junction composed of V and MgO layers. MgO tunnel barriers were recently found to significantly enhance the performance of magnetic tunnel junctions compared to an amorphous AlO barrier [5, 6]. MgO and V have good lattice matching (1.4% mismatch), even better than the magnetic counterparts [6]. These observations make V/MgO/V an attractive candidate for next-generation qubit applications. Below, however, we show that the normal-state conductance measurement suggests that this new system is prone to an interfacial electronic disorder and thus not suitable for qubit applications.

We took detailed four-point differential conductance measurements of these three systems above their superconducting transition temperatures, utilizing the differential conductance mode of a Keithley 6221 AC-current source and a Keithley 2182A nanovoltmeter. Interestingly, all three (even the most mundane p-Al/a-AlO/p-Al system) clearly showed non-trivial deviation from the standard WKB approximation. We found that analysis of these deviations from the WKB-like approximations reveals material-specific information related to the crystallinity of the tunnel barriers and the electronic quality of the interfaces.

2. Fabrication and processing

All three types of junctions were fabricated from trilayers grown without breaking vacuum. Standard optical lithography was then used to process them into tunnel junctions (area 70 μm^2) with four-point contacts as reported previously [3]. For p-Al/a-AlO/p-Al trilayers, the polycrystalline Al base layer was DC-sputtered at a rate of $\sim$50 nm min^{-1} in a high vacuum chamber (base pressure: low 10^{-6} Pa) at room temperature on sapphire substrates. Then the amorphous aluminum oxide layer was thermally grown at room temperature in 1500 Pa of ultrahigh purity oxygen in an oxidation chamber (base pressure: low 10^{-5} Pa) connected to the sputtering chamber. Finally, the top Al layer was DC-sputtered, again in the high vacuum sputtering chamber. These Al trilayer tunnel junctions are nominally identical to those used for previous qubit demonstrations [2]. The second system, e-Re/e-AlO/p-Al, was grown in an ultrahigh vacuum (UHV) (base pressure: 1×10^{-8} Pa) multi-chamber sputtering system equipped with a reflection high energy electron diffraction (RHEED) tool for *in situ* growth monitoring. Both the Re base layer and the AlO tunneling barrier were epitaxially grown on lattice-matched Al_2O_3 (0001) substrates at elevated temperatures, and the top Al layer was thermally evaporated from an effusion cell in a polycrystalline form at room temperature. The crystallinity of each layer was checked *in situ* by RHEED. The details of the vacuum system and the growth can be

found in earlier publications [3, 24]. This e-Re/e-AlO/p-Al system is also nominally identical to those previously used for demonstrating enhanced qubit performance [2, 23]. The third system, e-V/e-MgO/p-V, was grown in the same UHV chamber. The base V layer was DC-sputtered on lattice-matched MgO(001) substrates at $\sim$800 °C at a rate of $\sim$2 nm min^{-1}, and this condition led to single-crystalline epitaxial structures as confirmed by RHEED. After the film was cooled to room temperature, Mg was evaporated in 1.5×10^{-4} Pa of molecular oxygen to form the MgO tunnel barrier with a nominal thickness of 1.2 nm at a rate of $\sim$0.01 nm s^{-1}, and this MgO layer was fully epitaxial as grown. Such epitaxial growth of MgO at room temperature is quite different from that of the AlO tunnel barrier, which grows amorphous near the room temperature and requires high temperature annealing to form an epitaxial layer [3]. The strong tendency of the MgO layer toward epitaxy must be related to its simple crystal structure: the cubic rock-salt type. Then the top V layer was deposited by use of DC sputtering at room temperature in order to prevent thermal diffusion from happening through the tunnel barrier. Because of the room-temperature deposition, the top V layer turned out to be polycrystalline, as revealed by RHEED.

3. Junction: p-Al/a-AlO/p-Al

In figure 1(a) we show the differential conductance (dI/dV) measurements for a p-Al/a-AlO/p-Al junction taken at temperatures ranging from 170 to 4.2 K (above the T_C of Al). Overall, it exhibits a typical parabolic behavior in the broader bias range. However, as temperature decreases, a clear 'dimple' around zero bias develops for temperatures 106 K and below, within the $\pm$0.12 V region. A closer measurement of that region is shown in the top inset; note that for temperatures 106 K and below, the region around zero bias widens and flattens.

Another feature, shown more clearly in figures 1(b) and (c), is the oscillation in the differential conductance on top of the featureless parabolic background. Oscillations in conductance in aluminum tunnel junctions have been experimentally observed since the sixties [25–27]. Tunneling electrons can interact with the vibrational states of the ions, either at the interface between the metal and the oxide or in the tunnel barrier, showing increases in the differential conductance at specific voltages [1, 26, 28]. An effective phonon spectrum can be extracted from the d^2I/dV^2 curves [28], shown in figure 1(b), which clearly exhibit this oscillatory behavior.

To separate and enhance the oscillatory behavior, we used an arm fitting method [29]. In figure 1(c), graphs were normalized and divided by our highest available temperature (170 K) data that did not exhibit the oscillatory behavior. Here, three peaks can be identified on each side; if the peak voltage is plotted versus peak number, a near linear relation is obtained, as in figure 1(d), and this suggests harmonics of a single oscillator mechanism as its origin. Another noticeable feature is the dip around zero bias. At first, this feature may be reminiscent of the commonly observed ZBA, the suppression of density of states at zero bias due to disorder or electron–electron interactions [20, 21]. However, there is a clear difference; unlike other common ZBAs, which tend to develop further at lower temperatures, this dip feature does not get sharper at lower temperatures. Instead, as shown in the inset of figure 1(a), the conductance tends to flatten as the temperature drops toward the lowest temperature (4.2 K). This suggests that its origin must be something different from the common ZBA mechanism—the disorder or electron–electron interactions—and needs to be answered in future studies.

The main peak occurring at $\sim$0.10 V in d^2I/dV^2 has been observed before by other researchers and was interpreted as the Al–O stretching mode inside the aluminum oxide tunnel barriers [26, 30]. Surprisingly, however, both the higher harmonics and the zero bias feature have never been reported in p-Al/a-AlO/p-Al junctions, which are one of the most widely investigated superconducting tunnel junctions. The high quality of our trilayer junctions may have allowed observation of these elusive features; we generally find that the trilayer processed junctions exhibit better superconducting properties than other more conventionally processed junctions with *ex situ* steps between layers, which are prone to contamination at the interfaces.

Resistance measurements for this junction are shown in figure 1(e); the zero bias resistance versus temperature plot in this figure shows a saturation behavior at low temperatures, evidencing the absence of disorder-driven density-of-state suppression [14], as will be further discussed in section 5.

4. Junction: e-Re/e-AlO/p-Al

Figures 2(a) and (b) show the measurements for an e-Re/e-AlO/p-Al junction.

Conductance measurements in figure 2(a) were taken at 4.2 K. Unfortunately, all the junctions at higher temperatures became shorted, and therefore only 4.2 K data are available. Even partially crystalline AlO tunnel barriers were previously reported to be sensitive to high temperatures [30] and so this observation with our fully epitaxial AlO tunnel junctions may have been unavoidable. However, because measurements at high temperature are normally featureless, the lack of higher temperature data would not affect our main conclusions here.

The differential conductance plot, figure 2(a), clearly deviates from the parabolic behaviors expected from WKB models. Moreover, it differs significantly from that of the p-Al/a-AlO/p-Al system in multiple aspects. The most obvious difference is that the shape is very asymmetric, and this can be easily understood from the fact that the two electrodes (Re on one side and Al on the other) are different in this system. The second difference is the existence of kinks: two broad kinks at around 0.35 and −0.25 V, and sharper ones at around $\pm$0.01 V. Considering that these kinks are observed only in the epitaxial tunnel barrier system, they may be related to the crystallinity of the AlO tunnel barrier. Another subtle but critical difference from the p-Al/a-AlO/p-Al system is the absence of the Al–O vibration mode and its harmonics in this e-Re/e-AlO/p-Al system, although their tunnel barriers are different only in their crystallinity. This suggests two

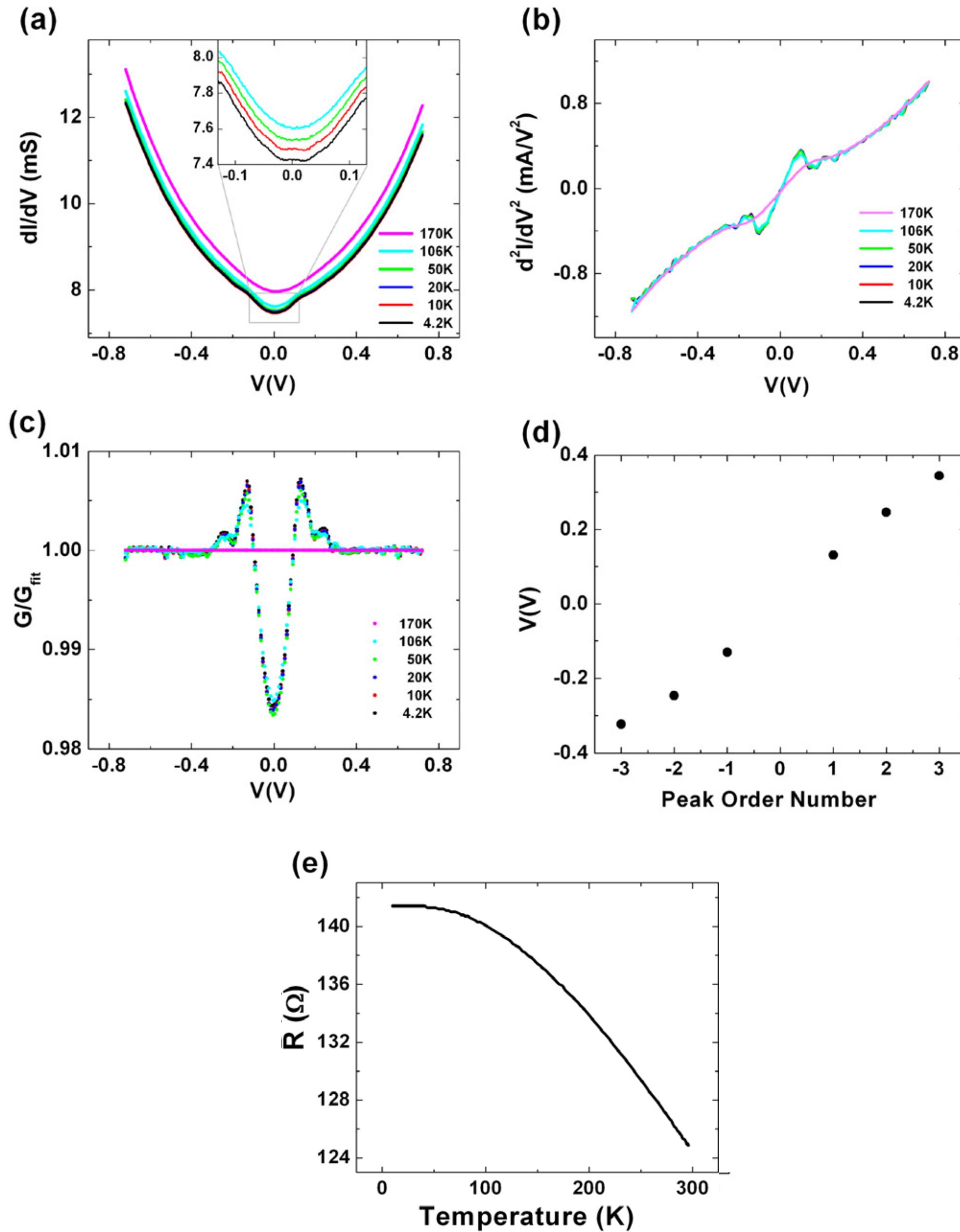

Figure 1. Measurements for the p-Al/a-AlO/p-Al junction. (a) Differential conductance (dI/dV or G) versus bias voltage measured at various temperatures from 170 K (top) to 4.2 K (bottom). Background near-parabolic shape is practically unchanged at all temperatures. However for temperatures 106 K and below, a 'dimple region' (around ± 0.12 V) around zero bias and small oscillations at higher biases, not clearly seen in these curves, develop. Inset: high-resolution dI/dV measurements of the 'dimple' region around zero bias; note that at the bottom of the dimple, a flat region develops below 20 K; 106 K (top) to 4.2 K (bottom). (b) Second derivative curves (d^2I/dV^2) of the conductance data from part (a). Maxima can be observed at $\sim$0.10, 0.22, and 0.30 V for both positive and negative bias. (c) Normalized conductance divided by the best parabolic arm fit of the 170 K graph; oscillatory behaviors are clearly visible. (d) Peak voltage versus peak order number. Peak voltages are almost linear, suggesting a common mechanism of harmonics. (e) Resistance at zero bias versus temperature; a saturation point is reached at low temperatures, indicating standard tunneling as the main mechanism.

possibilities. The first is that the presumed Al–O vibration mode may in fact be related to some other resonance channel such as an O–H vibration, considering that the O–H mode also has matching energy scales at values similar to the Al–O mode [1, 28, 30, 31]. In such a case, the enhanced conductance at the characteristic voltages might not be intrinsic to the AlO tunnel barrier but more due to impurities. However, it is hard to believe that the only vibration mode in the AlO tunnel junctions created without breaking high vacuum is not the Al–O channel but some other impurity channel. The second and more likely scenario is that the Al–O vibration mode is related to the amorphous structure of the tunnel barrier and thus is missing in the epitaxial AlO barrier. A similar observation was also made previously even in partially crystalline AlO tunnel barriers [30]. Finally, it will be an interesting question for future studies whether the absence of Al–O vibration mode in the epitaxial AlO tunnel barrier is also related to the suppression of two-level fluctuators in the

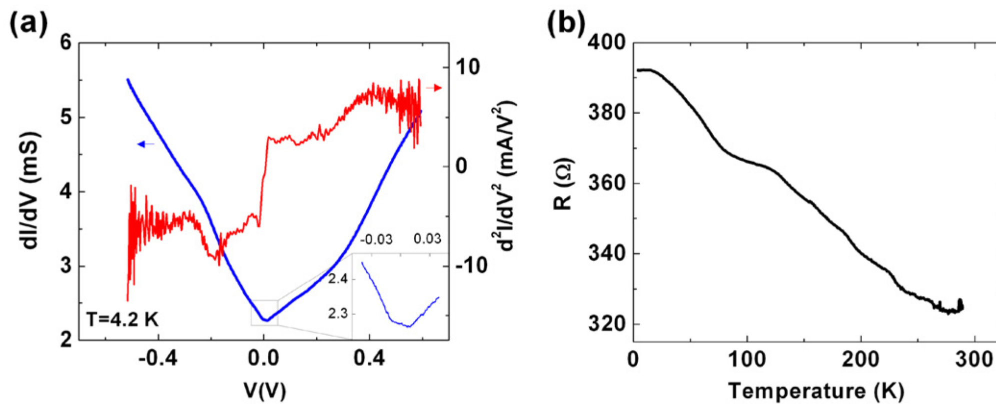

Figure 2. Measurements for the e-Re/e-AlO/p-Al junction. (a) $\mathrm{d}I/\mathrm{d}V$ versus bias voltage at 4.2 K (blue graph); asymmetry and a number of kinks are evident. $\mathrm{d}^2I/\mathrm{d}V^2$ plot (red graph); unlike that of the p-Al/a-AlO/p-Al junction, oscillatory behaviors are absent here. Inset: additional detailed $\mathrm{d}I/\mathrm{d}V$ measurement taken at 4.2 K within ± 0.05 V region; the sharp kinks at ± 0.01 V and the asymmetric flat at around zero bias are noticeable. (b) Resistance at zero bias versus temperature measurement; the resistance saturates at low temperatures, indicating standard tunneling as the dominant mechanism.

epitaxial barrier compared to its amorphous counterpart, as observed in previous studies [2, 23].

The resistance measurement in figure 2(b) reaches a saturation level at low temperatures, and this is consistent with the flattening of the differential conductance around zero bias, indicating electronically clean interfaces similar to the p-Al/a-AlO/p-Al system.

5. Junction: e-V/e-MgO/p-V

In figure 3(a), we plot the differential conductance measured at temperatures ranging from 270 to 6.4 K (above the vanadium T_{C} of 5.4 K) for the e-V/e-MgO/p-V junction. At 270 K, our highest measurement temperature for this junction, the behavior is clearly parabolic, with a very good fit (not shown) with the BDR model. However, as the temperature is lowered, the parabolic behavior gradually transforms to V-shaped curves, as depicted in the figure. The gradual transition from parabolic to linear behavior, which is typical of the common ZBA, can be seen more clearly in figure 3(b), where the curves are all normalized to the values around ± 0.15 V. Such a transition from parabolicity to sharp ZBA was obtained previously in other systems [14, 32], and is regarded as a sign of electronic disorder at the interface. In comparison, although figure 2(a) might also give the impression of a similar ZBA, even for the e-Re/e-AlO/p-Al junction, the inset of figure 2(a) shows that there is in fact a flat, albeit asymmetric, region right around zero voltage.

At high temperatures, because many of the interactions are washed out by thermal smearing, the plot of conductance versus voltage can be well fitted by the non-interacting WKB model. However, once the temperature drops below the energy scales of these interactions, the WKB approximation breaks down and anomalous behaviors show up, as seen in all of our three junction types. Although not all these anomalies are fully understood, there exist a number of theoretical models trying to explain some of these features. For example, electron–electron interactions for low-dimensional electron systems lead to logarithmically vanishing density-of-states (DOS) near the Fermi level when impurities interfere with the electron–electron interactions [20]. Because the differential conductance is proportional to DOS, vanishing DOS at zero bias will appear as suppression of the tunneling conductance at low temperatures, deviating from the standard parabolicity at higher temperatures. These predictions are consistent with previous experiments where irradiated tunnel junctions showed increasing ZBA effect as the irradiation level increased, which is equivalent to increasing disorder in the tunnel junctions [16]. $G(V)/G(V)_{270\ \mathrm{K}}$ (plot shown in figure 3(c)) is consistent with this picture and is also similar to the behavior predicted for the average DOS in a 2D electron gas for a low disordered electron system, as proposed by Bartosch and Kopietz [22]. The only slight difference is that instead of logarithmic divergence near zero bias, our system shows linear dependence, not only in figure 3(c) but also in the temperature dependence of figure 3(d). This linear dependence is more consistent with the model in [31].

Unlike the other two junctions, the zero bias resistance of the e-V/e-MgO/p-V junction kept increasing down to the lowest temperature in figure 3(d). This is consistent with the electronic disorder picture described for the $\mathrm{d}I/\mathrm{d}V$ measurements. The most likely origin of this electronic disorder is the oxidation of vanadium at the interfaces. It is well known that vanadium and many other transition metals can easily form bad metals when exposed to oxygen, and that is part of the reason why native oxides of these metals cannot be used as reliable tunnel barriers. Even if we observed sharp single-crystalline interfaces from RHEED during growth between the bottom vanadium and the MgO tunnel barrier, we cannot rule out the possibility of vanadium getting partially oxidized at the interface. Such oxidation can lead to a disordered electronic state as observed here. Although not presented here, we also measured the current versus voltage of these e-V/e-MgO/p-V junctions at 100 mK in a dilution refrigerator, but no superconducting gap was observed even if the vanadium electrodes were superconducting. This implies

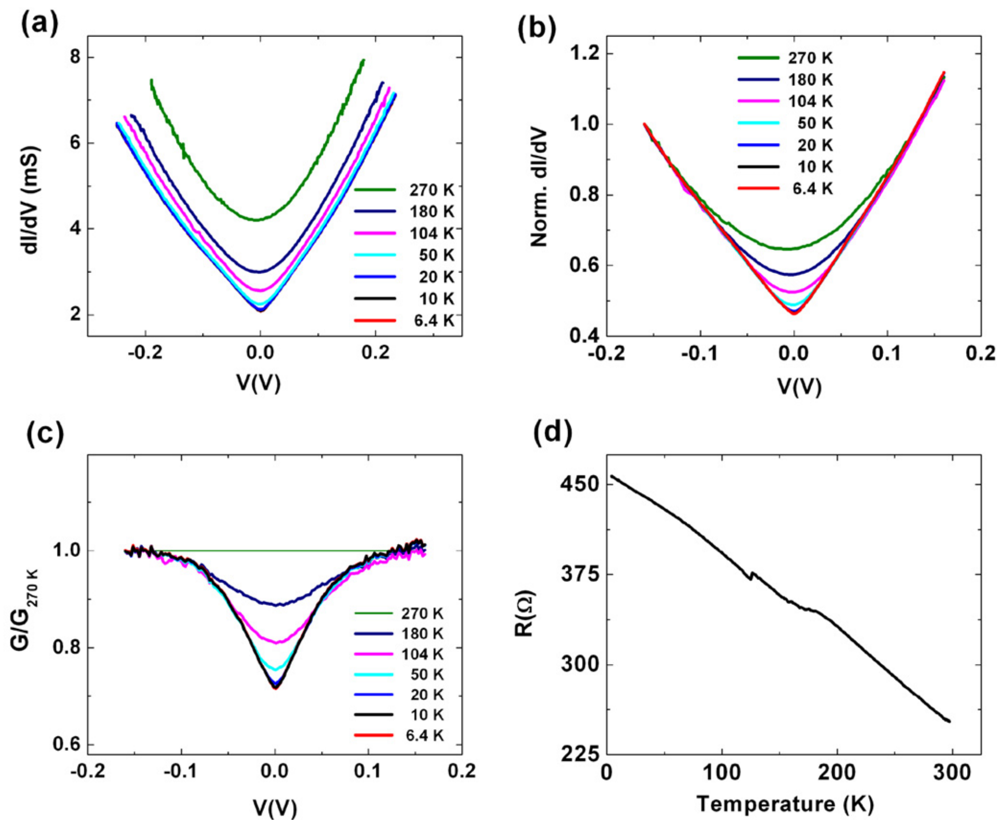

Figure 3. Measurements for the e-V/e-MgO/p-V junction. (a) Tunneling conductance (dI/dV) versus bias voltage, measured at temperatures ranging from 270 K (top) to 6.4 K (bottom). Parabolic behavior at high temperatures gradually changes to linear ZBA at low temperatures. (b) Normalized dI/dV curves for figure 3(a), showing the temperature evolution more clearly. (c) Conductance (G) curves of part (a), normalized, and divided by the highest temperature (270 K) data; at the lowest temperatures, the linear suppression of the conductance below the high temperature parabolic background is clear. (d) Resistance at zero bias versus temperature measurement; unlike the other two junctions, resistance does not saturate at low temperatures. Instead, it increases almost linearly down to the lowest temperature, indicating that some temperature-dependent interaction mechanism is active beyond standard tunneling.

that the interfacial electronic disorder, which is responsible for the ZBA, also resulted in poor superconducting junction properties. This is in stark contrast to the e-Re/e-AlO/p-Al case, where the base Re layer remains electronically clean even if it is exposed to molecular oxygen at a similar level to the e-V/e-MgO/p-V case [2, 3, 23]. Based on these observations, e-V/e-MgO/p-V junctions will not be suitable for qubit applications, unless a new growth scheme is developed to prevent the oxidation of the V layers.

6. Conclusions

We measured the normal-state conductance for three different tunnel junctions: p-Al/a-AlO/p-Al, e-Re/e-AlO/p-Al, and e-V/e-MgO/p-V. For the first and third junctions, measurements taken near room temperature were well fitted to the standard WKB model parabolic behavior. However, all three junctions showed significant deviations from the parabolicity at cryogenic temperatures. In the p-Al/a-AlO/p-Al junction we found that the interaction between electrons and the Al–O vibration modes leads to characteristic oscillations in the voltage-dependent differential conductance. In the e-Re/e-AlO/p-Al junction we found that the Al–O vibration mode is absent, suggesting a close connection between the Al–O vibration channel and the crystallinity of the AlO barrier. In the e-V/e-MgO/p-V junction we observed suppression of the DOS, and it can be accounted for by electronic disorder at the interfaces due to oxidation of the vanadium layer. This implies that preventing oxidation of the vanadium layer is an essential step to make the e-V/e-MgO/p-V junction a viable solution for qubit applications. This work shows that simple normal-state measurements can provide ample information for the development of new tunnel junctions in superconducting qubit applications.

Acknowledgments

This work was supported by the Institute for Advanced Materials and Devices (IAMDN), Department of Physics and Astronomy of Rutgers University, Intelligence Advanced Research Projects Activity (IARPA) and BBN, and is a contribution of the US Government, not subject to copyright.

References

[1] Burstein E and Lundqvist S 1969 *Tunneling Phenomena in Solids: Lectures* (New York: Plenum)

[2] Oh S, Cikac K, Kline J S, Silampaa M A, Osborn K D, Whittaker J D, Simmonds R W and Pappas D P 2006 *Phys. Rev.* B **74** 100502(R)
[3] Oh S, Cicak K, McDermott R, Cooper K B, Osborn K D, Simmonds R W, Steffen M, Martinis J M and Pappas D P 2005 *Supercond. Sci. Technol.* **18** 1396
[4] Simmonds R W, Lang K M, Hite S N, Pappas D P and Martinis J M 2004 *Phys. Rev. Lett.* **93** 077003
[5] Parkin S S P, Kaiser C, Panchula A, Rice P M, Hughes B, Samant M and Yang S-H 2004 *Nat. Mater.* **3** 862
[6] Yuasa S, Nagahama T, Fukushima A, Suzuki Y and Ando K 2004 *Nat. Mater.* **3** 868
[7] Simmons J G 1963 *J. Appl. Phys.* **34** 1793
[8] Simmons J G 1964 *J. Appl. Phys.* **35** 2655
[9] Harrison W A 1961 *Phys. Rev.* **123** 85
[10] Brinkman W F, Dynes R C and Rowell J M 1970 *J. Appl. Phys.* **41** 1915
[11] Miller C W, Li Z-P, Schuller I V, Dave R W, Slaughter J M and Akerman J 2006 *Phys. Rev.*. B **74** 212404
[12] Miller C W, Li Z-H, Akerman J and Schuller I K 2007 *Appl. Phys. Lett.* **90** 043513
[13] Altshuler B L and Aronov A G 1979 *Solid State Commun.* **30** 115
[14] O'Donnell J, Andrus A E, Oh S, Colla E V and Eckstein J N 2000 *Appl. Phys. Lett.* **76** 1914
[15] Rowell J M and Shen L Y 1966 *Phys. Rev. Lett.* **17** 15
[16] Mora N A, Bermon S and Loferski J J 1971 *Phys. Rev. Lett.* **27** 664
[17] Adler G J and Straus J 1976 *Phys. Rev.* B **13** 1377
[18] Americh-Humet X and Serra-Mestres F 1979 *Phys. Status Solidi* **54** 655
[19] Hall R N, Racette J H and Ehrenreich H 1960 *Phys. Rev. Lett.* **4** 456
[20] Altshuler B L, Aronov A G and Lee P A 1980 *Phys. Rev. Lett.* **44** 1288
[21] Lee P A and Ramakrishnan T V 1985 *Rev. Mod. Phys.* **57** 287
[22] Bartosch L and Kopietz P 2002 *Eur. Phys. J.* B **28** 29
[23] Kline J S, Wang H, Oh S, Martinis J and Pappas D P 2009 *Supercond. Sci. Technol.* **22** 015004
[24] Oh S, Hite D, Cicak D A, Osborn K D, Simmonds R W, McDermott R, Cooper K B, Steffen M, Martinis J M and Pappas D P 2006 *Thin Solid Films* **496** 389
[25] Raven M S 1986 *Phys. Scr.* T **14** 93
[26] Moodera J S, Nowak J and van de Veerdonk R J M 1998 *Phys. Rev. Lett.* **80** 2941
[27] Jaklevich R C and Lambe J 1966 *Phys. Rev. Lett.* **17** 1139
[28] Wolf E L 1985 *Principles of Electron Tunneling Spectroscopy* (New York: Oxford University Press)
[29] Oliver B and Nowak J 2004 *J. Appl. Phys.* **95** 546
[30] Liehr M and Ewert S 1983 *Z. Phys.* B **52** 95
[31] Shklovskii B I and Efros A L 1984 *Electronic Properties of Doped Semiconductors* (New York: Springer)
[32] Magnus F *et al* 2007 *Appl. Phys. Lett.* **91** 122106